


**Non-Hermitian BCS-BEC evolution with a complex scattering length**

M. Iskin

*Department of Physics, Koç University, Rumelifeneri Yolu, 34450 Sarıyer, Istanbul, Turkey* (Received 3 February 2020; revised 2 January 2021; accepted 7 January 2021; published 22 January 2021)

Having both elastic and inelastic two-body processes that are characterized by a complex  $s$ -wave scattering length between  $\uparrow$  and  $\downarrow$  fermions in mind, here we apply the non-Hermitian extension of the mean-field theory to the BCS-BEC evolution at zero temperature. We construct the phase diagram of the system, where we find a reentrant superfluid (SF) transition that is intervened by a normal and/or a metastable phase as a function of increasing inelasticity. This transition occurs in a large parameter regime away from the unitarity, i.e., on both the BCS and BEC sides of the resonance, and it is mostly governed by the exceptional points. In addition, except for the strongly inelastic regime, we also show that the SF phase can be well described by the condensation of weakly interacting bosonic pairs in the two-body bound state with a complex binding energy.

DOI: [10.1103/PhysRevA.103.013724](https://doi.org/10.1103/PhysRevA.103.013724)**I. INTRODUCTION**

The presence of magnetically tunable Feshbach resonances in ultracold collisions permits the ground state of a superfluid (SF) Fermi gas to evolve from the BCS limit of weakly bound and largely overlapping Cooper pairs to the Bose-Einstein condensate (BEC) limit of strongly bound and small overlapping bosonic molecules [1–3]. For this purpose, since the main objective is to understand the effects of elastic collisions between particles, one customarily chooses a purely real scattering length, and tunes both its magnitude and sign across the resonance; i.e., first the scattering length takes small and negative values in the BCS limit, then it diverges and changes sign at the resonance, and then it takes small and positive values in the BEC limit. In the case of an  $s$ -wave resonance, this evolution turned out to be a crossover phenomenon without a phase transition anywhere in between.

Motivated by the recent works on non-Hermitian fermionic superfluidity [4–7], and particularly by Ref. [7] on the Hubbard model with a complex-valued interaction strength, here we study the non-Hermitian extension of the BCS-BEC evolution with a complex  $s$ -wave scattering length between  $\uparrow$  and  $\downarrow$  fermions in a continuum model, whose real (imaginary) part describes the elastic (inelastic) processes [8,9]. Our self-consistent mean-field theory for the ground state is almost identical to that of Ref. [7], except that we allow not only the SF order parameter but also the chemical potential to take complex values. At the expense of this complication, our number equation becomes purely real, and our theory accurately reproduces the two-body physics with a complex binding energy in the BEC limit [10].

Some of our primary findings can be summarized as follows. By constructing the phase diagram of the continuum model, we first reveal a reentrant SF transition that is intervened by a normal and/or a metastable phase as a function of increasing inelasticity. In contrast to the lattice model where a similar transition is reported only in the weakly bound BCS

regime [7], our model exhibits a reentrant transition not only on the BCS side of the resonance but also on the strongly bound BEC side except for the crossover region around unitarity. Then, in the weakly inelastic region, we show that the BEC side can be well described by the condensation of weakly interacting bosonic pairs in the two-body bound state with a complex binding energy. However, the physics differs considerably in the strongly inelastic region, where the SF phase is a many-body phenomenon.

The rest of the paper is organized as follows. In Sec. II, we first introduce the non-Hermitian extension of the mean-field Hamiltonian, and then obtain the self-consistency equations under the notion of biorthogonal quantum mechanics. In Sec. III, we present the phase diagram of the system, and discuss the self-consistent solutions for the SF order parameters and the chemical potentials. The paper ends with a brief summary of our findings in Sec. IV and an Appendix on the use of complex scattering parameters in collision physics.

**II. MEAN-FIELD THEORY**

In this paper, we consider the situation where the contact density-density interaction  $U$  between  $\uparrow$  and  $\downarrow$  fermions has an imaginary component, i.e.,  $U = U_R + iU_I$  with  $U_R \geq 0$  and  $U_I \geq 0$  [7]. The physical motivation for the inclusion of such a term into the effective Hamiltonian is due to the inelastic two-body loss processes, and it can be derived from the quantum master equation with the proper Lindbladian operator [7,11–15]. While the master equation with the quantum-recycle term describes the dissipative dynamics of the system at all times, our effective Hamiltonian describes only the short-time dynamics during which the recycle term is assumed to be negligible. As proposed in Ref. [13], a complex-valued interaction can effectively be realized with cold atoms through postselection (i.e., projecting out the quantum jumps) by a continuous monitoring of the particle number.

### A. Mean-field Hamiltonian

When  $U$  is a complex number, the effective mean-field Hamiltonian for the stationary Cooper pairs can be written as [7]

$$H_{\text{emf}} = \sum_{\mathbf{k}} (c_{\mathbf{k}\uparrow}^\dagger \quad c_{-\mathbf{k}\downarrow}) \begin{pmatrix} \xi_{\mathbf{k}} & \Delta \\ \bar{\Delta} & -\xi_{\mathbf{k}} \end{pmatrix} \begin{pmatrix} c_{\mathbf{k}\uparrow} \\ c_{-\mathbf{k}\downarrow}^\dagger \end{pmatrix}, \quad (1)$$

where  $c_{\mathbf{k}\sigma}^\dagger$  ( $c_{\mathbf{k}\sigma}$ ) creates (annihilates) a spin- $\sigma$  fermion with momentum  $\mathbf{k}$ , and  $\xi_{\mathbf{k}} = \epsilon_{\mathbf{k}} - \mu$  with  $\epsilon_{\mathbf{k}} = \hbar^2 k^2 / (2m)$  the usual free-particle dispersion in continuum and  $\mu$  the chemical potential. Unlike its Hermitian counterpart, it turns out that  $\mu = \mu_R + i\mu_I$  must have an imaginary component in order for the number equation to take purely real values [10]. In addition, the complex parameters  $\bar{\Delta} \neq \Delta^*$  are the non-Hermitian extension of the SF order parameter for pairing.

In this paper, we are interested in the ground state of the system at zero temperature that is based on the notion of biorthogonal quantum mechanics as follows [16]. First of all, given that  $H_{\text{emf}}^\dagger \neq H_{\text{emf}}$  is a non-Hermitian Hamiltonian, its right ground state is not the same as the left one. Analogous to the usual BCS theory, one can write  $|\text{BCS}\rangle = \prod_{\mathbf{k}} (u_{\mathbf{k}} + v_{\mathbf{k}} c_{\mathbf{k}\uparrow}^\dagger c_{-\mathbf{k}\downarrow}^\dagger) |0\rangle$  for the right ground state and  $\langle\langle \text{BCS} | = \langle 0 | \prod_{\mathbf{k}} (u_{\mathbf{k}} + \bar{v}_{\mathbf{k}} c_{-\mathbf{k}\downarrow} c_{\mathbf{k}\uparrow})$  for the left one [7]. In accordance with the biorthogonal formalism, these coefficients must satisfy  $u_{\mathbf{k}}^2 + v_{\mathbf{k}} \bar{v}_{\mathbf{k}} = 1$  for every  $\mathbf{k}$ , so that the inner product  $\langle\langle \text{BCS} | \text{BCS} \rangle = 1$  is normalized to unity [16]. This leads to  $u_{\mathbf{k}} = \sqrt{(E_{\mathbf{k}} + \xi_{\mathbf{k}}) / (2E_{\mathbf{k}})}$  and  $v_{\mathbf{k}} = -\sqrt{\Delta(E_{\mathbf{k}} - \xi_{\mathbf{k}}) / (2\bar{\Delta}E_{\mathbf{k}})}$  for the right ground state, and to  $\bar{v}_{\mathbf{k}} = -\sqrt{\bar{\Delta}(E_{\mathbf{k}} - \xi_{\mathbf{k}}) / (2\Delta E_{\mathbf{k}})}$  for the left one, where the quasiparticle energy  $E_{\mathbf{k}} = \sqrt{\xi_{\mathbf{k}}^2 + \Delta \bar{\Delta}}$  is a complex number in general, and may host the so-called exceptional points in  $\mathbf{k}$  space.

### B. Exceptional points

Unlike the Hermitian Hamiltonians that give rise to a real eigenspectrum in an orthonormal eigenspace, the complex eigenspectrum and eigenvectors of non-Hermitian Hamiltonians may coalesce into one at the so-called exceptional points in the parameter space; i.e., they correspond to the degenerate points in a non-Hermitian system [17,18]. Thus, in sharp contrast to a degeneracy in the real spectrum of Hermitian systems, a degeneracy in the complex spectrum of non-Hermitian systems makes the Hamiltonian matrix defective; i.e., it does not have a complete basis of eigenvectors, and it is not diagonalizable. Since many of the novel properties and applications of non-Hermitian systems have been attributed to the presence of these points, next we analyze them for our system.

Let us consider a generic two-band Bloch Hamiltonian of a non-Hermitian system that is governed by the Hamiltonian matrix  $H_{\mathbf{k}} = d_{0\mathbf{k}} \tau_0 + \mathbf{d}_{\mathbf{k}} \cdot \boldsymbol{\tau}$ , where  $\tau_0$  is a  $2 \times 2$  identity matrix,  $\boldsymbol{\tau} = (\tau_x, \tau_y, \tau_z)$  is a vector of Pauli matrices, and  $\mathbf{d}_{\mathbf{k}} = \mathbf{d}_{R\mathbf{k}} + i\mathbf{d}_{I\mathbf{k}}$  parametrizes, respectively, the Hermitian and anti-Hermitian terms. The eigenvalues of this Hamiltonian matrix can be written as  $E_{s,\mathbf{k}} = d_{0\mathbf{k}} + s\sqrt{d_{R\mathbf{k}}^2 - d_{I\mathbf{k}}^2 + 2i\mathbf{d}_{R\mathbf{k}} \cdot \mathbf{d}_{I\mathbf{k}}}$ , where  $s = \pm$ , and its exceptional points occur when the conditions  $d_{R\mathbf{k}}^2 = d_{I\mathbf{k}}^2$  and  $\mathbf{d}_{R\mathbf{k}} \cdot \mathbf{d}_{I\mathbf{k}} = 0$  are simultaneously satisfied [19,20]. Here  $d_{R\mathbf{k}}$  and  $d_{I\mathbf{k}}$  are the magnitudes of the cor-

responding vectors. For our Hamiltonian, we set  $d_{0\mathbf{k}} = 0$ , and choose the gauge  $\Delta = (\Delta_R + i\Delta_I)e^{i\theta}$  and  $\bar{\Delta} = (\Delta_R + i\Delta_I)e^{-i\theta}$  [7], leading to  $\mathbf{d}_{R\mathbf{k}} = (\Delta_R \cos \theta, -\Delta_R \sin \theta, \epsilon_{\mathbf{k}} - \mu_R)$  and  $\mathbf{d}_{I\mathbf{k}} = (\Delta_I \cos \theta, -\Delta_I \sin \theta, -\mu_I)$ . Thus, the exceptional points occur when the conditions  $\Delta_R^2 + (\epsilon_{\mathbf{k}} - \mu_R)^2 = \Delta_I^2 + \mu_I^2$  and  $\Delta_R \Delta_I = \mu_I(\epsilon_{\mathbf{k}} - \mu_R)$  are simultaneously satisfied. Assuming  $\mu_I < 0$  (i.e., see our numerical results below), these conditions reduce to  $\mu_I = -\Delta_R$  and  $\epsilon_{\mathbf{k}} = \mu_R - \Delta_I$ , and they correspond to a surface of exceptional points when  $\mu_R > 0$ .

### C. Self-consistency equations

In terms of the right and left ground states, the SF order parameters can be written as the expectation values of the pair annihilation and creation operators where  $\Delta = U \sum_{\mathbf{k}} \langle\langle c_{\mathbf{k}\uparrow} c_{-\mathbf{k}\downarrow} \rangle\rangle$  and  $\bar{\Delta} = U \sum_{\mathbf{k}} \langle\langle c_{-\mathbf{k}\downarrow}^\dagger c_{\mathbf{k}\uparrow}^\dagger \rangle\rangle$ . They both lead to the order parameter equation  $1/U = \sum_{\mathbf{k}} 1/(2E_{\mathbf{k}})$  [7], where  $\langle\langle c_{\mathbf{k}\uparrow} c_{-\mathbf{k}\downarrow} \rangle\rangle = u_{\mathbf{k}} v_{\mathbf{k}}$  and  $\langle\langle c_{-\mathbf{k}\downarrow}^\dagger c_{\mathbf{k}\uparrow}^\dagger \rangle\rangle = u_{\mathbf{k}} \bar{v}_{\mathbf{k}}$ . Here we follow the usual BCS-BEC crossover approach [21], and substitute  $1/U = -mV/(4\pi \hbar^2 a_s) + \sum_{\mathbf{k}} 1/(2\epsilon_{\mathbf{k}})$ , where  $V$  is the volume, and the  $s$ -wave scattering length  $a_s = a_R + ia_I$  between  $\uparrow$  and  $\downarrow$  fermions in vacuum is a complex number with  $a_I < 0$  when  $U_I > 0$ . See the Appendix for their connection to the physical parameters. Similarly, the number of particles can be obtained from the expectation value of the number operator where  $N = \sum_{\mathbf{k}\sigma} \langle\langle c_{\mathbf{k}\sigma}^\dagger c_{\mathbf{k}\sigma} \rangle\rangle$ . This leads to the number equation  $N = \sum_{\mathbf{k}} (1 - \xi_{\mathbf{k}}/E_{\mathbf{k}})$  [7], where  $\langle\langle c_{\mathbf{k}\sigma}^\dagger c_{\mathbf{k}\sigma} \rangle\rangle = \bar{v}_{\mathbf{k}} v_{\mathbf{k}}$ . Unless we allow  $\mu$  to have complex values, the imaginary component of  $N = N_R + iN_I$  is nonzero in general [10]. This may not be surprising given that the Hermitian operators do not correspond to physical observables in the biorthogonal quantum mechanics, causing their expectation values to be not necessarily real.

Noting that the SF order parameters always appear as  $\Delta \bar{\Delta}$  in the self-consistency equations, we choose a special gauge above satisfying  $H_{\text{emf}}^\dagger = H_{\text{emf}}^*$ , and set  $\Delta \bar{\Delta} = \Delta_0^2$  where  $\Delta_0 = \Delta_R + i\Delta_I$  is a complex number [7]. To make further progress, we also introduce a simpler notation  $\xi_{\mathbf{k}}^2 + \Delta_0^2 = A_{\mathbf{k}} + iB_{\mathbf{k}}$  where  $A_{\mathbf{k}} = (\epsilon_{\mathbf{k}} - \mu_R)^2 + \Delta_R^2 - \mu_I^2 - \Delta_I^2$  and  $B_{\mathbf{k}} = 2\Delta_I \Delta_R - 2\mu_I(\epsilon_{\mathbf{k}} - \mu_R)$ , and define  $|E_{\mathbf{k}}| = (A_{\mathbf{k}}^2 + B_{\mathbf{k}}^2)^{1/4}$  and the principal value  $\phi_{\mathbf{k}} = \text{atan2}(B_{\mathbf{k}}, A_{\mathbf{k}}) \in (-\pi, +\pi]$ . Note that having a branch cut along the negative  $A_{\mathbf{k}}$  axis [22] guarantees a positive value for the real part of  $E_{\mathbf{k}}$ . This allows us to decouple the two complex self-consistency equations into four real ones:

$$-\frac{mVa_R}{4\pi \hbar^2 |a_s|^2} = \sum_{\mathbf{k}} \left[ \frac{\cos(\phi_{\mathbf{k}}/2)}{2|E_{\mathbf{k}}|} - \frac{1}{2\epsilon_{\mathbf{k}}} \right], \quad (2)$$

$$-\frac{mVa_I}{4\pi \hbar^2 |a_s|^2} = \sum_{\mathbf{k}} \frac{\sin(\phi_{\mathbf{k}}/2)}{2|E_{\mathbf{k}}|}, \quad (3)$$

$$\frac{k_F^3 V}{3\pi^2} = \sum_{\mathbf{k}} \left[ 1 - \frac{(\epsilon_{\mathbf{k}} - \mu_R) \cos(\phi_{\mathbf{k}}/2) - \mu_I \sin(\phi_{\mathbf{k}}/2)}{|E_{\mathbf{k}}|} \right], \quad (4)$$

$$0 = \sum_{\mathbf{k}} \frac{(\epsilon_{\mathbf{k}} - \mu_R) \sin(\phi_{\mathbf{k}}/2) + \mu_I \cos(\phi_{\mathbf{k}}/2)}{|E_{\mathbf{k}}|}. \quad (5)$$

Here,  $|a_s| = \sqrt{a_R^2 + a_I^2}$  is the magnitude of  $a_s$ ,  $N_R$  is set to its noninteracting value  $k_F^3 V / (3\pi^2)$  with  $k_F$  the Fermi wave vector, and  $N_I$  is set to zero.

We note that our formalism recovers the usual BCS-BEC crossover problem by construction [21], i.e.,  $\Delta_I \rightarrow 0$ ,  $\mu_I \rightarrow 0$ , and  $\phi_{\mathbf{k}} \rightarrow 0$  in the limit when  $U_I \rightarrow 0$  or equivalently  $1/(k_F a_I) \rightarrow -\infty$ . The  $a_I \rightarrow 0^-$  limit has been well studied in the past [1–3], for which case the mean-field theory provides a qualitative understanding of the ground state in the entire range of  $-\infty < 1/(k_F a_R) < \infty$ . Hoping that the non-Hermitian extension of the mean-field theory is also valid, i.e., at least for the weakly inelastic region where  $1/(k_F a_I) \lesssim -5$  if not for the strongly inelastic region where  $1/(k_F a_I) \gtrsim -2$  or the extremely inelastic limit when  $1/(k_F a_I) \rightarrow 0^-$ , next we resort to a fully numerical approach, and analyze the effects of a finite  $1/(k_F a_I)$  on the SF properties.

### III. NUMERICAL RESULTS

After iterating Eqs. (2)–(5) for self-consistent solutions of  $\Delta_R$ ,  $\Delta_I$ ,  $\mu_R$ , and  $\mu_I$ , we construct the phase diagram that is shown in Fig. 1. The diagram involves three phases that are characterized by the following criteria [7]. In the green regions denoted as “normal,” our numerical calculations do not converge to a self-consistent solution with a finite  $\Delta_R \neq 0$  and/or  $\Delta_I \neq 0$ . While we find convergent solutions with a reliable accuracy in both the white regions denoted as “metastable” and the yellow region denoted as “superfluid,” these regions are distinguished by the sign of the real part of the condensation energy. Here, the condensation energy  $E_c = \Delta_0^2 / U - \sum_{\mathbf{k}} (E_{\mathbf{k}} - \sqrt{\xi_{\mathbf{k}}^2}) = -\sum_{\mathbf{k}} (E_{\mathbf{k}} - \sqrt{\xi_{\mathbf{k}}^2})^2 / (2E_{\mathbf{k}})$  corresponds to the energy difference between the SF and normal phases, and its positive (negative) real part suggests a metastable (stable)

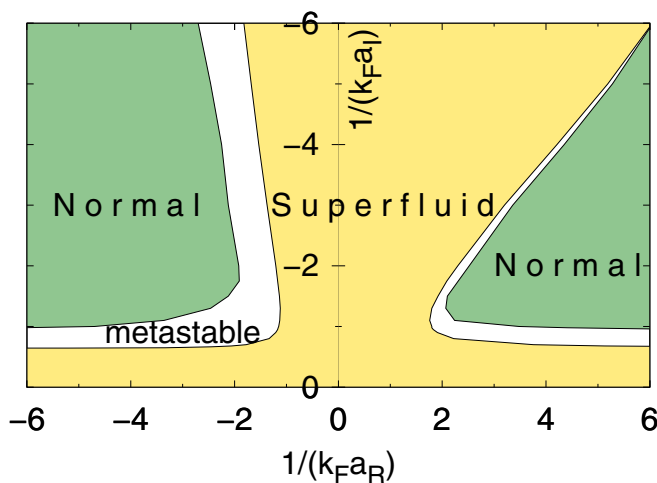


FIG. 1. The phase diagram at zero temperature. In the green normal regions, our numerical calculations do not converge reliably to a self-consistent solution with a nontrivial  $\Delta_R \neq 0$  and/or  $\Delta_I \neq 0$ . In the white metastable regions, the condensation energy of the SF solution does not correspond to the global minimum of the real part of the energy; i.e., the nontrivial solutions are energetically stable only in the yellow SF region.

SF solution; i.e., the SF solution is a local (global) minimum of the real part of the energy.

In Fig. 1, we have two disconnected normal regions. The one on the BCS side of the resonance, i.e., when  $1/(k_F a_R) < 0$ , is quite similar in structure to the recent work on the lattice model [7]: There is a reentrant SF transition that is intervened by a normal and/or a metastable phase as a function of increasing  $1/(k_F a_I)$  from  $-\infty$  towards  $0^-$ . We find that the conditions  $A_{\mathbf{k}} = 0$  and  $B_{\mathbf{k}} = 0$  (or equivalently  $\mu_I = -\Delta_R < 0$  with  $\mu_R > 0$ ) are simultaneously satisfied on the periphery of the normal region, and, therefore, the normal region is attributed entirely to the presence of exceptional points in the energy spectrum. When  $1/(k_F a_I) \lesssim -2$ , we noticed that  $\min A_{\mathbf{k}}$  is negative (positive) in the metastable (SF) region, and that the energetic-stability boundary coincides very well with the condition  $\min A_{\mathbf{k}} = 0$  or simply  $\Delta_R^2 = \Delta_I^2 + \mu_I^2$  in our continuum model. In connection to this, we also observe that the momentum distribution, that is given by the summand  $[\dots]$  of Eq. (4), of the metastable phase is not strictly bounded by zero from below and by 2 from above in a tiny  $\mathbf{k}$ -space region near the Fermi momentum. However, curiously enough, the Pauli principle is not violated on the energetically stable side in the SF region.

On the other hand, the normal region on the BEC side of the resonance, i.e., when  $1/(k_F a_R) > 0$ , has no counterpart in the lattice model [7]. We believe this difference is quite intuitive given the distinct nature and properties of the tightly bound bosonic pairs in these models. In the lattice model, the pairs become strongly repulsive when they are on the same site, due to the important role played by the Pauli exclusion principle [23]. In sharp contrast, the pairs become weakly repulsive in the continuum model [21]. As the real part of the pair-pair scattering length  $a_{p,R} \propto a_R$  gets weaker with increasing  $1/(k_F a_R)$ , the SF phase eventually gives way to the normal phase once the imaginary part  $a_{p,I} \propto a_I$  of the pair-pair scattering length dominates over  $a_{p,R}$ . In particular, in the weakly inelastic region when  $1/(k_F a_I) \lesssim -5$ , we note that the transition from the SF phase to the normal one occurs approximately at  $1/(k_F a_R) \approx 1/(k_F a_I)$  without a sizable metastable region in between.

This motivates us to study the two-body binding problem with a complex  $a_s$ . Similar to the expression for the usual two-body problem with a real  $a_s$ , the complex binding energy  $\varepsilon_b$  of the two-body bound state is determined by  $1/U = \sum_{\mathbf{k}} 1/(2\varepsilon_{\mathbf{k}} - \varepsilon_b)$ , leading to  $\varepsilon_b = -\hbar^2/(m a_s^2)$ . Here, we eliminate  $1/U$  in favor of  $a_s$  via the relation given in Sec. II C, and perform the integral over real  $k$  using the residue theorem after going to the complex  $k \rightarrow z$  plane. Even though the final result is identical in mathematical form to the usual problem with a real  $a_s$ , here  $\varepsilon_b = \varepsilon_R + i\varepsilon_I$  is a complex number in general where  $\varepsilon_R = \hbar^2(a_I^2 - a_R^2)/(m|a_s|^4)$  and  $\varepsilon_I = 2\hbar^2 a_I a_R / (m|a_s|^4)$ . Therefore, we conclude that a two-body bound state occurs only when  $a_R > 0$  and  $a_R > |a_I|$ , leading to  $\varepsilon_R < 0$  and  $\varepsilon_I < 0$ , and its lifetime is determined by  $\tau_b = -\hbar/(2\varepsilon_I)$ . See the Appendix for further discussion. The absence of a two-body bound state clearly explains why the SF region is bounded by  $1/(k_F a_R) < 1/(k_F |a_I|)$  on the BEC side of the resonance for the weakly inelastic region when  $1/(k_F a_I) \lesssim -5$ .

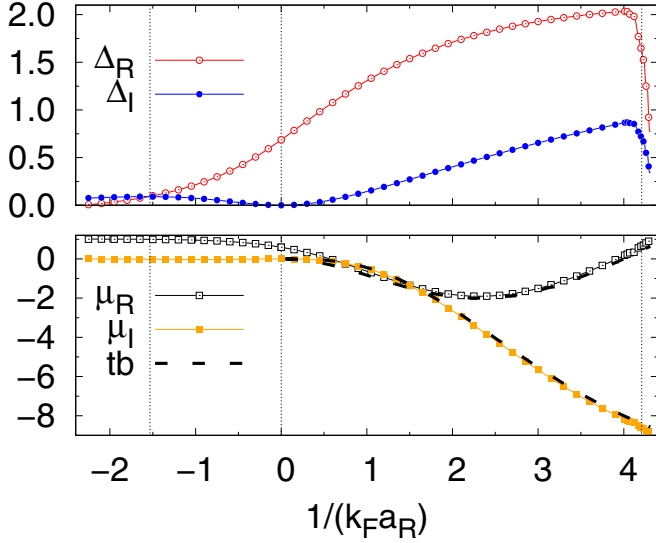


FIG. 2. Self-consistent solutions for  $1/(k_F a_I) = -4$  in units of  $\epsilon_F$ . The vertical lines are guides to the eye for the locations of the phase transitions, and the dashed lines are the real and imaginary parts of the two-body result  $\epsilon_b/2$ .

In order to gain more physical insight into the phase diagram, we set  $1/(k_F a_I)$  to  $-4$  in Fig. 2, and present the resultant self-consistent solutions as a function of  $1/(k_F a_R)$ . The numerical energy scale is the Fermi energy,  $\epsilon_F = \hbar^2 k_F^2 / (2m)$ . First of all, independently of the value of  $1/(k_F a_I)$ , both  $\Delta_I$  and  $\mu_I$  vanish precisely at the resonance when  $1/(k_F a_R) = 0$ . For this reason, the evolutions of  $\Delta_I$  and  $\mu_I$  are non-monotonous in the BCS-BEC crossover region. Although it is not visible in Fig. 2,  $\mu_I$  is negative and has the shape of an inverted bell curve. In the weakly inelastic region when  $1/(k_F a_I) \lesssim -5$ , we find that while  $\mu_R \rightarrow \epsilon_F$  and  $\mu_I \rightarrow 0^-$  in the BCS limit, they approach the two-body binding energy  $\mu_R \rightarrow \epsilon_b/2$  and  $\mu_I \rightarrow \epsilon_I/2$  in the BEC limit. This is clearly seen in Fig. 2 where the dashed lines correspond to  $\mu = \epsilon_b/2$ . Thus, similar to the BEC side of the usual BCS-BEC crossover problem [21], we conclude that the SF phase here can also be well described by the condensation of weakly interacting bosonic pairs in the two-body bound state.

On the other hand, the physics differs considerably in the strongly inelastic region especially when  $1/(k_F a_I) \gtrsim -2$ . To illustrate this, we set  $1/(k_F a_I)$  to  $-1$  in Fig. 3, and present the resultant self-consistent solutions as a function of  $1/(k_F a_R)$ . We find not only that  $\mu_R > \epsilon_F$  is above the Fermi energy and  $\mu_I < 0$  is nonvanishing in the BCS limit, but they also deviate substantially from the two-body result in the BEC limit. We note that, given the absence of a two-body bound state when  $1/(k_F a_R) > 1/(k_F |a_I|)$ , the SF phase here is a many-body phenomenon just like the BCS side. Furthermore, in the extremely inelastic limit when  $1/(k_F a_I) \rightarrow 0^-$ , we find that  $\Delta_R \approx 0.69\epsilon_F$ ,  $\Delta_I \rightarrow 0$ ,  $\mu_R \approx 0.59\epsilon_F$ , and  $\mu_I \rightarrow 0$  for the entire range of  $1/(k_F a_R)$ . It suggests that a unitary Fermi SF can be achieved by  $k_F a_I \rightarrow -\infty$  even in the  $k_F a_R \rightarrow 0^-$  limit. Whether this amusing result is an indication that the non-Hermitian extension of the mean-field theory eventually breaks down in the vicinity of a resonance when  $k_F a_I \rightarrow -\infty$

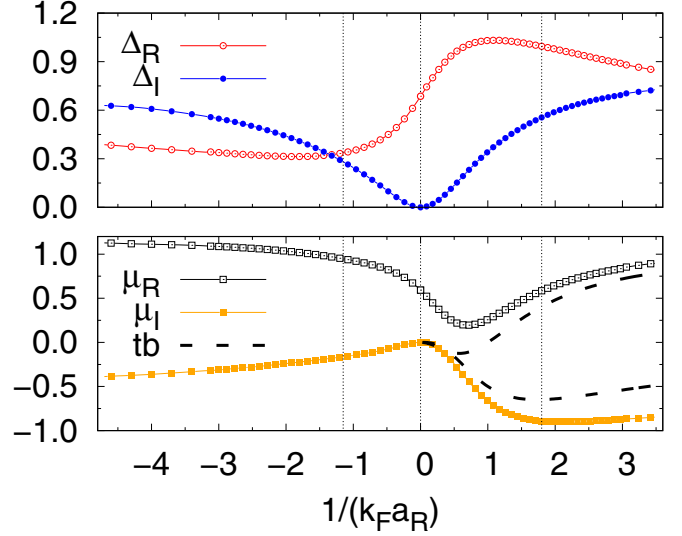


FIG. 3. Self-consistent solutions for  $1/(k_F a_I) = -1$  in units of  $\epsilon_F$ . The vertical lines are guides to the eye for the locations of the phase transitions, and the dashed lines are the real and imaginary parts of the two-body result  $\epsilon_b/2$ .

deserves further investigation. This is because it is analogous to the recent observation where strong inelastic collisions were shown to inhibit particle losses, and drove a one-dimensional Bose gas into a dissipative but long-lived strongly correlated Tonks-Girardeau regime through fermionization of the bosons [11,12,24]. While similar results were reported both in continuum and lattice systems, the equivalence between strong dissipation and a Pauli exclusion principle was interpreted as a manifestation of the continuous quantum Zeno effect only in the lattice case [11,24]. See also Ref. [14] for a similar conclusion and interpretation in the context of fractional quantum Hall states. We also note that the condition  $\mu_I = -\Delta_R$  with  $\mu_R > 0$  is satisfied only in the nearly flat normal boundary around  $1/(k_F a_I) \gtrsim -1$ , and, therefore, only this portion of the boundary can be attributed to the presence of exceptional points in the energy spectrum.

#### IV. CONCLUSION

In summary, here we discussed the non-Hermitian extension of the BCS-BEC evolution with a complex  $s$ -wave scattering length  $a_s = a_R + ia_I$  between  $\uparrow$  and  $\downarrow$  fermions. Our self-consistent mean-field theory for the ground state is almost identical to the recent literature [7], except that we allow not only the SF order parameter  $\Delta_0$  but also the chemical potential  $\mu$  to take complex values [10]. This turned out to be one of the crucial ingredients of the theory in the strongly bound BEC regime where  $2\mu$  approaches the binding energy  $\epsilon_b = -\hbar^2 / (ma_s^2)$  of the two-body bound state in vacuum.

Some of our primary findings can be summarized as follows. We constructed the phase diagram of the system, where we found a reentrant SF transition that is intervened by a normal and/or a metastable phase as a function of increasing  $1/(k_F a_I)$  from  $-\infty$  towards  $0^-$ . This transition occurs in a large parameter window of  $1/(k_F a_R)$  away from the unitarity, i.e., both on the BCS and BEC sides of the resonance, and it

is entirely (partially) governed by the exceptional points when  $a_R < 0$  ( $a_R > 0$ ). Furthermore, in the weakly inelastic region when  $1/(k_F a_I) \lesssim -5$ , we showed that the BEC side of the resonance can be well described by the condensation of weakly interacting bosonic pairs in the two-body bound state with a complex  $\varepsilon_b$ . However, the physics differs considerably in the strongly inelastic region especially when  $1/(k_F a_I) \gtrsim -2$ , where the SF phase is a many-body phenomenon reminiscent of the BCS side. As an outlook, the validity of the mean-field theory deserves particular investigation in the extremely inelastic limit when  $1/(k_F a_I) \rightarrow 0^-$ . In addition, it is important to go beyond the non-Hermitian Hamiltonian, and consider the full Lindblad dynamics of the dissipative SF through, e.g., a time-dependent mean-field formalism [25].

#### ACKNOWLEDGMENTS

The author thanks A. L. Subaşı for discussions, and acknowledges funding from TÜBİTAK, Grant No. 11001-118F359.

#### APPENDIX: RESONANCE SCATTERING WITH A COMPLEX SCATTERING LENGTH

Complex scattering lengths have been widely used in scattering theory, and they can be achieved and even measured in multichannel scattering or optical Feshbach resonances. However, it turns out that the resonance becomes much less prominent when the imaginary part becomes strong, limiting the tunability of the real part of the scattering length. See Sec. II A 3 in Ref. [9] for a detailed discussion of the theory and the analysis of the experimental results.

In particular, our theoretical parameters  $a_R$  and  $a_I$  can be directly related to the physical ones that are discussed in Ref. [9] as follows. In terms of the collision parameters, the complex  $s$ -wave scattering length  $a_s$  is parametrized as

$$a_s = a - ib = a_{bg} + a_{bg} \frac{\Gamma_0}{-E_0 + i\gamma/2} \quad (\text{A1})$$

with the imaginary component  $b > 0$  characterizing the inelastic scattering of atoms. Here  $a_{bg}$  is the background scattering length representing the off-resonant value,  $\Gamma_0$  is the resonance strength,  $E_0$  is the threshold resonance position, and  $\gamma/\hbar$  is the decay rate for the decay of the bound state into all available loss channels in the  $k \rightarrow 0$  limit. The sign of  $\Gamma_0$  is

the same as the sign of  $a_{bg}$  and it can be either positive or negative. This leads to [9]

$$a = a_{bg} - a_{bg} \frac{\Gamma_0 E_0}{E_0^2 + \gamma^2/4}, \quad (\text{A2})$$

$$b = a_{bg} \frac{\Gamma_0 \gamma}{2E_0^2 + \gamma^2/2}, \quad (\text{A3})$$

showing that  $a$  attains its maximum variation of  $a_{bg} \pm a_{bg} \Gamma_0/\gamma$  at  $E_0 = \pm\gamma/2$ , where  $b = a_{bg} \Gamma_0/\gamma$ . While a quasisubbound state occurs when  $a > a_{bg}$  or  $E_0 < 0$ , it may not be possible to tune  $a$  at will when  $\gamma$  is not weak [9]. This is because as the resonance is induced by the bound state getting close to the scattering threshold, it becomes much less prominent given that the bound state is no longer well defined. In addition,  $b$  attains its peak value when  $a - a_{bg}$  changes sign [9].

On the other hand, the decay rate  $\gamma$  can be written as

$$\gamma = \frac{2a_{bg} \Gamma_0 b}{(a - a_{bg})^2 + b^2}, \quad (\text{A4})$$

showing that  $\gamma$  attains (for a given  $a - a_{bg}$ ) its maximum value of  $a_{bg} \Gamma_0/b$  at  $b = a - a_{bg}$ . In particular, we note that while  $b \neq 0$  is the origin of the dissipation of the bound state, a large  $b$  does not lead to a strong dissipation. More importantly, by reexpressing it as  $\gamma = -(2a_{bg}^2 \Gamma_0^2/E_0)b(a - a_{bg})/[(a - a_{bg})^2 + b^2]^2$ , and then matching this expression with the inverse lifetime  $\hbar/\tau_b = -2\varepsilon_I = -4\hbar^2 a_I a_R/[m(a_R^2 + a_I^2)^2]$  of our two-body bound state, we find that  $a_R$  plays the role of  $a - a_{bg}$  and  $a_I$  plays the role of  $-b$  in the region when  $a - a_{bg} > 0$ . This is indeed consistent with our finding that  $a_R > 0$  is one of the requirements for the creation of a two-body bound state.

Even though we introduced the theoretical parameters  $a_R$  and  $a_I$  to characterize the imaginary interaction strength between particles in our effective non-Hermitian Hamiltonian, and varied them freely in constructing the resultant phase diagram of the system, it is clear that these parameters are not independent from each other in cold-atom collisions. Given that Fig. 1 covers the entire phase space, we hope the correspondence discussed above may be used to gain physical intuition about physical systems once the relevant parameters of a certain setup are specified.

[1] *Ultra-Cold Fermi Gases*, Proceedings of the International School of Physics ‘‘Enrico Fermi,’’ Course CLXIV, edited by M. Inguscio, W. Ketterle, and C. Salomon (IOS Press, Amsterdam, 2008).  
 [2] S. Giorgini, L. P. Pitaevskii, and S. Stringari, Theory of ultracold atomic Fermi gases, *Rev. Mod. Phys.* **80**, 1215 (2008).  
 [3] For a very recent review, see G. C. Strinati, P. Pieri, G. Röpke, P. Schuck, and M. Urban, The BCS-BEC crossover: From ultracold Fermi gases to nuclear systems, *Phys. Rep.* **738**, 1 (2018).  
 [4] A. Ghatak and T. Das, Theory of superconductivity with non-Hermitian and parity-time reversal symmetric Cooper pairing symmetry, *Phys. Rev. B* **97**, 014512 (2018).

[5] L. Zhou and X. Cui, Enhanced fermion pairing and superfluidity by an imaginary magnetic field, *iScience* **14**, 257 (2019).  
 [6] N. Okuma and M. Sato, Topological Phase Transition Driven by Infinitesimal Instability: Majorana Fermions in Non-Hermitian Spintronics, *Phys. Rev. Lett.* **123**, 097701 (2019).  
 [7] K. Yamamoto, M. Nakagawa, K. Adachi, K. Takasan, M. Ueda, and N. Kawakami, Theory of Non-Hermitian Fermionic Superfluidity with a Complex-Valued Interaction, *Phys. Rev. Lett.* **123**, 123601 (2019).  
 [8] T. Köhler, E. Tiesinga, and P. S. Julienne, Spontaneous Dissociation of Long-Range Feshbach Molecules, *Phys. Rev. Lett.* **94**, 020402 (2005).

- [9] C. Chin, R. Grimm, P. Julienne, and E. Tiesinga, Feshbach resonances in ultracold gases, *Rev. Mod. Phys.* **82**, 1225 (2010).
- [10] Even in the case of a half-filled lattice model that is considered in Ref. [7], our numerical calculations show that setting the real chemical potential  $\mu$  to zero gives a nonzero, but negligible, imaginary contribution to the number equation. Having a real  $\mu$  turns out to be problematic in the case of our continuum model, and we circumvent around it by allowing a complex  $\mu$ . In return, our theory captures the two-body physics with a complex binding energy when the fermion pairs form tightly bound bosonic molecules.
- [11] J. J. García-Ripoll, S. Dürr, N. Syassen, D. M. Bauer, M. Lettner, G. Rempe, and J. I. Cirac, Dissipation-induced hard-core boson gas in an optical lattice, *New J. Phys.* **11**, 013053 (2009).
- [12] S. Dürr, J. J. García-Ripoll, N. Syassen, D. M. Bauer, M. Lettner, J. I. Cirac, and G. Rempe, Lieb-Liniger model of a dissipation-induced Tonks-Girardeau gas, *Phys. Rev. A* **79**, 023614 (2009).
- [13] Y. Ashida, S. Furukawa, and M. Ueda, Quantum critical behavior influenced by measurement backaction in ultracold gases, *Phys. Rev. A* **94**, 053615 (2016).
- [14] T. Yoshida, K. Kudo, and Y. Hatsugai, Non-Hermitian fractional quantum Hall states, *Sci. Rep.* **9**, 16895 (2019).
- [15] T. Liu, J. J. He, T. Yoshida, Z.-L. Xiang, and F. Nori, Non-Hermitian topological Mott insulators in one-dimensional fermionic superlattices, *Phys. Rev. B* **102**, 235151 (2020).
- [16] D. C. Brody, Biorthogonal quantum mechanics, *J. Phys. A: Math. Theor.* **47**, 035305 (2014).
- [17] M. V. Berry, Physics of nonhermitian degeneracies, *Czech. J. Phys.* **54**, 1039 (2004).
- [18] W. D. Heiss, Exceptional points of non-Hermitian operators, *J. Phys. A: Math. Gen.* **37**, 2455 (2004).
- [19] R. Okugawa and T. Yokoyama, Topological exceptional surfaces in non-Hermitian systems with parity-time and parity-particle-hole symmetries, *Phys. Rev. B* **99**, 041202(R) (2019).
- [20] J. C. Budich, J. Carlström, F. K. Kunst, and E. J. Bergholtz, Symmetry-protected nodal phases in non-Hermitian systems, *Phys. Rev. B* **99**, 041406(R) (2019).
- [21] J. R. Engelbrecht, M. Randeria, and C. A. R. Sá de Melo, BCS to Bose crossover: Broken-symmetry state, *Phys. Rev. B* **55**, 15153 (1997).
- [22] See <https://en.wikipedia.org/wiki/Atan2> for a description of the function atan2.
- [23] M. Iskin and C. A. R. Sá de Melo, Quantum phases of Fermi-Fermi mixtures in optical lattices, *Phys. Rev. A* **78**, 013607 (2008).
- [24] N. Syassen, D. M. Bauer, M. Lettner, T. Volz, D. Dietze, J. J. Garcia-Ripoll, J. I. Cirac, G. Rempe, and S. Dürr, Strong dissipation inhibits losses and induces correlations in cold molecular gases, *Science* **320**, 1329 (2008).
- [25] K. Yamamoto, M. Nakagawa, N. Tsuji, M. Ueda, and N. Kawakami, Collective excitations and nonequilibrium phase transition in dissipative fermionic superfluids, [arXiv:2006.06169](https://arxiv.org/abs/2006.06169).